control region. Expression of some other cancer-related genes may also be inhibited by methylation.

Silencing of the suppressor of cytokine signaling-1 (SOCS-1; also known as SSI-1 or JAB) is a member of the SOCS protein family. It switches off cytokine signaling by directly interacting with Janus kinase (JAK) proteins; its expression renders cells unresponsive to interleukin-6 stimulation.[12] The SH2 domain of SOCS-1 binds to a JH1 domain of JAK2 and inhibits its phosphorylation, downregulating the JAK/STAT pathway.[12,13] SOCS-1 inhibits the biological effects of cytokines in vivo; its forced expression interrupts macrophage differentiation induced by IL-6 and suppresses CD23 expression induced by IL-4.[12,13] Thus, SOCS-1 modulates the immune system through interacting with the cytokine network.

Recently, *SOCS-1*-deficient mice have been shown to die within 3 weeks after birth from a myeloproliferative disorder resulting from unbridled interferon (IFN)-γ and tumor necrosis factor (TNF)-α signaling.[14] As a negative regulator of cytokine signaling, *SOCS-1* is now a candidate gene for inactivating mutations that will favor the development of malignancies; SOCS-1 may inhibit cell proliferation induced by oncogenic forms of other known SOCS-1-interacting proteins. In addition to the results in hematopoietic neoplasia, recently suppression of SOCS-1 expression has been reported in HCC, in which the CpG-rich domain in the coding region of *SOCS-1* was found to be aberrantly methylated.[15] However, in general, it is the methylation of the 5′ non-coding region, which contains the promoter, but not that of the coding region, which determines gene expression.[16,17] We therefore conducted this experiment to evaluate the methylation status of the *SOCS-1* in HCC by methylation-specific PCR (MSPCR) using primers located both in the 5′-noncoding region and in the CpG-rich domain (CpG island) of the coding region.

Patients and methods

Patients

We studied 22 patients (19 males and 3 females; median age, 63.5 years) with HCC who had underlying chronic hepatitis C with or without cirrhosis (8 without and 14 with cirrhosis), all of whom underwent hepatectomy between 1997 and 2000 at the University of Tokyo Hospital. This study was approved by the ethics review committee of the institute, and carried out in accordance with the World Medical Association Helsinki Declaration, adopted in 1964 and amended in 1996. Informed consent was obtained from each patient. All the patients were positive for anti-hepatitis C virus (HCV) confirmed by the second-generation enzyme immunoassay and HCV-RNA by reverse-transcriptase-polymerase chain reaction (RT-PCR), and none were positive for serum hepatitis B surface antigen (HBsAg). The clinicopathological features of the patients are shown in Table 1.

Tissue samples and cell lines

The cancerous (HCC) and noncancerous (non-HCC) liver tissue samples obtained from these patients were fixed in 10% formalin for hematoxylin and eosin staining, or immediately frozen and stored at −80°C until further use. The histological staging of the noncancerous tissues was performed according to the European classification for chronic hepatitis,[18] and that of cancerous tissue was based on the TNM classification.[19] All the 22 tumors were classified as advanced HCCs: 5 well-, 14 moderately, and 3 poorly differentiated HCCs (see Table 1). Human HCC cell lines PLC/PRF/5, HuH-7, and the B-cell line, BJAB, were obtained from the American Type Culture Collections. The cells were grown in Dulbecco's modified Eagle's medium (DMEM) supplemented with 10% fetal bovine serum.

DNA preparation and bisulfite treatment

Genomic DNA was extracted from the frozen tissues by standard proteinase K digestion and phenol/chloroform extraction.[20] Then, bisulfite modification of genomic DNA was carried out as described previously[21] with slight modification. Briefly, DNA (1 μg) in a volume of 20 μl was denatured by NaOH at a final concentration at 0.3 M for 15 min at 37°C. Then, 113 μl 3.6 M sodium bisulfite (Sigma-Aldrich, St. Louis, MO, USA) at pH 5 and 7.2 μl 10 mM hydroquinone (Sigma-Aldrich), both freshly prepared, were added and mixed well. Then, the samples were incubated under mineral oil at 95°C for 15 min followed by incubation at 50°C for 4 h, and this cycle was repeated 15 times. Modified DNA was purified and resuspended in 50 μl water. The modification was completed by adding NaOH at a final concentration of 0.3 M for 5 min at room temperature, after which ethanol precipitation was carried out.

Genomic and methylation-specific PCR (MSPCR)

Bisulfite-modified and unmodified DNA was subjected to amplification using the PCR method. Primers used for the PCR in the current study are shown in Table 2. Amplification was carried out in a thermal cycler for a total of 35 cycles consisting of 95°C for 30 s, 60°C for 30 s, and 30 s at 72°C in 50 μl reaction mixture containing 200 mM deoxynucleoside triphosphates (dNTPs), 1.0 mM of each primer, and 1× PCR buffer [16.6 mM

Table 1. SOCS-1 gene methylation and clinicopathological findings of 22 hepatocellular carcinoma (HCC) patients

		Methylation of SOCS-1							
		CpG island				5′-noncoding			
		M[a]		U[a]		M[a]		U[a]	
	n	HCC	nHCC	HCC	nHCC	HCC	nHCC	HCC	nHCC
Sex									
Male	19	7	1	1	4	10	2	5	9
Female	3	2	0	0	1	2	0	0	1
Cirrhosis									
−	8	2	0	0	1	3	0	2	4
+	14	7	1	1	4	9	3	3	5
Pathology of HCC[b]									
WD	5	3	0	0	2	3	0	1	3
MD	14	4	1	1	2	7	1	3	6
PD	3	2	0	0	1	2	1	1	0
Tumor size (cm)									
<2	5	2	0	0	0	2	2	2	1
≥2	17	7	1	1	5	10	0	3	9
Vascular invasion									
Absent	19	8	1	1	4	11	2	5	9
Present	3	1	0	0	1	1	0	0	1
Distant metastasis[c]									
M0	20	9	1	1	4	12	1	4	10
M1	2	0	0	0	1	0	1	1	0
Stage grouping[c]									
I	4	1	0	0	0	1	2	2	1
II	5	3	0	0	2	3	0	1	2
III	11	4	1	0	3	6	1	2	7
IV	2	1	0	1	0	2	0	0	0
Overall	22	9* (41%)	1* (5%)	1* (5%)	5* (23%)	12* (55%)	2* (9%)	5* (23%)	10* (46%)

[a]M, hypermethylated pattern; U, unmethylated pattern; not all samples were informative for methylation status
[b]WD, well-differentiated; MD, moderately differentiated; PD, poorly differentiated
[c]According to TNM classification
*$P < 0.01$ when the association of HCC and methylation was judged by Fisher's exact test for each of CpG island and 5′-noncoding region

Table 2. Polymerase chain reaction (PCR) primers used in the current study

	Sequence	Position
Forward		
HM1F	TTCGCGTGTATTTTTAGGTCGGTC	(400–423)
HM2F	GAGTATTCGCGTGTATTTTTAGG	(395–417)
UM1F	TTATGAGTATTTGTGTGTATTTTTAGGTTGGTT	(391–423)
UM2F	TGAGTATTTGTGTGTATTTTTAGG	(394–417)
UMPF-M	GTTCGGTTTCGTTTAGTTTTCGAGG	(−708–684)
UMPF-U	GTTTGGTTTTGTTTAGTTTTTGAGG	(−708–684)
Reverse		
HM1R	CGACACAACTCCTACAACGACCG	(537–559)
UM1R	CACTAACAACACAACTGGTACAACAACCA	(537–565)
UM2R	CAACACAACTCCTACAACAACCA	(543–565)
UMPR-M	ACCCCGACCGACCGCGATCTC	(−590–570)
UMPR-U	ACCCCAACCAACCACAATCTC	(−590–570)

ammonium sulfate, 67mM Tris-HCl (pH 8.8), 6.7mM $MgCl_2$, 10mM 2-mercaptoethanol, and 0.001% (w/v) gelatin] and 1.25 units of Ampli-Taq polymerase (Perkin-Elmer Cetus, Norwalk, CT, USA). The PCR products were separated in a 2.0% agarose gel and visualized by staining with ethidium bromide.

Reverse transcription (RT)-PCR

Total RNA was extracted from cells using RNAzolB (TEL-TEST, Friendswood, TX, USA). Three micrograms of total RNA were reverse transcribed by Superscript II (Gibco-BRL, Gaithersburg, MD, USA) using oligo(dT) primer and subjected to PCR. Primers for RT-PCR of SOCS-1 gene expression were as follows: forward, 5′-CACGCACTTCCGCACATTCC-3′; reverse, 5′-TCCAGCAGCTCGAAGAGGCA-3′. For the RT-PCR, the quantity of cDNA template and the number of amplification cycles were optimized to ensure that the reaction was terminated during the linear phase of product amplification, so that semiquantitative comparisons of the mRNA abundance between different samples were possible. RT-PCR with glyceraldehyde phosphate dihydrogenase (GAPDH) primers was done to adjust the amounts of RNA in each experiment.

Statistical analysis

Fisher's exact test was used for statistical evaluation, and P values below 0.05 were considered significant.

Results

Methylation status of SOCS-1 in cultured cell lines

First, the methylation status of the CpG island in the coding region of *SOCS-1* was analyzed in cell lines by MSPCR using the primer sets, HM1F+HM1R and UM1F+UM1R, according to the method of Yoshikawa et al.[15] MSPCR using these primers, however, could not determine the methylation status of the gene: the use of the primers resulted in dimer formation without methylation- or unmethylation-specific bands. We therefore redesigned new sets of primers located in the CpG island of *SOCS-1* (Table 2; HM2F+HM1R for detecting a methylation-specific band and UM2F+UM2R for an unmethylation-specific band). MSPCR with these sets of primers enabled successful detection of methylation- and unmethylation-specific bands in PLC/PRF/5 cells (Fig. 1). The unmethylation-specific band alone was detected in HuH-7 cells, in agreement with the previous report.[15]

Analysis using the primers located in the 5′-noncoding region (see Table 2) yielded a similar pattern, excluding that there were both methylation- and unmethylation-specific bands also in HuH-7 cells (Fig. 1). Accordingly, the primer sets HM2F+HM1R and UM2F+UM2R were used for the analysis of the methylation status of the CpG island, and UMPF-M+UMPR-M and UMPF-U+UMPR-U were used for the 5′-noncoding region, thereafter.

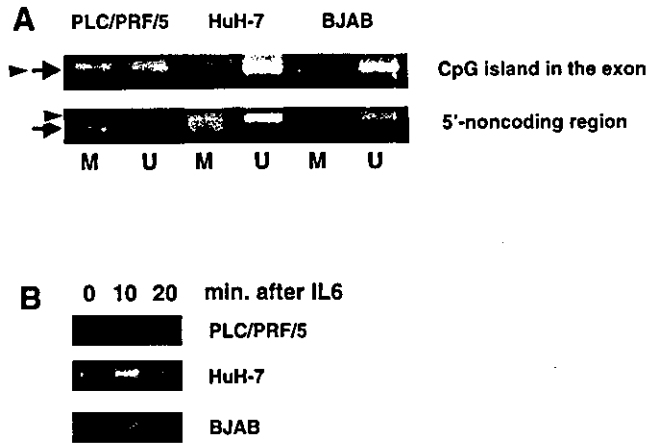

Fig. 1. Genomic and methylation-specific (MSPCR) analysis of cultured hepatoma cell lines in the CpG island and 5′-no-coding region of the *SOCS-1* gene. DNA from human hepatoma cell lines, PLC/PRF/5 and HuH-7, and a B-cell line, BJAB, was analyzed by MSPCR after bisulfite treatment as described in the Patients and methods section. **A** MSPCR with the primers in the CpG island and those in the 5′-noncoding region. **B** RT-PCR showing the expression of SOCS-1 in cell lines before and after the addition of IL-6 (10ng/ml). The *arrow* indicates the position of the methylation-specific band; the *arrowhead* indicates the position of the unmethylation-specific band. *M*, MSPCR with methylation-specific primers; *U*, MSPCR with unmethylation-specific primers

Expression of SOCS-1 mRNA in cell lines

The expression of SOCS-1 was determined by semiquantitative RT-PCR. Although SOCS-1 expression was abundant in HuH-7 and BJAB cells in the baseline and was enhanced by the addition of IL-6 (10ng/ml), only marginal expression and no enhancement were detected in PLC/PRF/5 cells. These results are consistent with the methylation status that was determined in the current study and with the expression status in the baseline that was observed in a previous report.[15]

Methylation status of SOCS-1 in human tumor samples

Then, DNA extracted from human HCC and non-HCC tissues was tested for the methylation status of the *SOCS-1* by MSPCR. Only 10 and 6 tissue samples were informative for determining a methylation-specific band

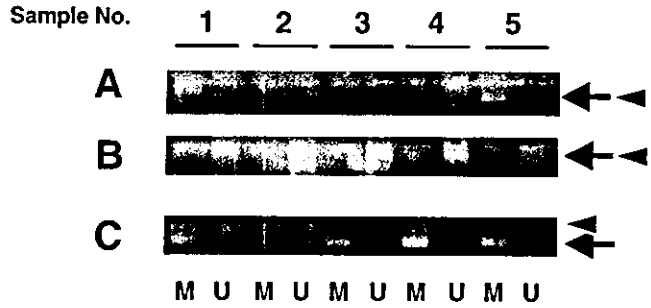

Fig. 2. MSPCR analysis of the CpG island and 5′-noncoding region of the *SOCS-1* from 22 HCC tissue samples. With the same primers used in Fig. 1, 22 pairs of HCC and non-HCC samples were analyzed by MSPCR. Representative cases are shown. Samples *1* and *2* were well-differentiated HCC, *3* and *4* were moderately differentiated HCC, and *5* was poorly differentiated HCC. Panel **B** shows their non-HCC counterparts. **A** MSPCR of DNA from HCC tissue samples with the primers in CpG island. **B** MSPCR of DNA from non-HCC tissue samples with the primers in CpG island. **C** MSPCR of DNA from HCC tissue samples with the primers in 5′-noncoding region. The *arrow* indicates the position of the methylation-specific band; the *arrowhead* indicates the position of the unmethylation-specific band HCC, hepatocellular carcinoma; M, MSPCR with methylation-specific primers; U, MSPCR with unmethylation-specific primers

and an unmethylation-specific band, respectively, when the primers in the CpG island were used. In 9 HCC tissue samples the band indicative of aberrant methylation in the CpG island was detected, while the band indicating unmethylation was detected in 1 HCC tissue sample (Fig. 2). In contrast, in the corresponding non-HCC tissue samples, only 1 exhibited the methylation pattern, whereas the unmethylation pattern was observed in 5 non-HCC tissue samples. Thus, aberrant methylation of *SOCS-1* was significantly associated with HCC rather than with non-HCC tissues ($P = 0.0076$ by Fisher's exact test).

Using primers in the 5′-noncoding promoter region, 14 and 15 HCC tissue samples were informative for a methylation-specific band and an unmethylation-specific band, respectively. Aberrant methylation was observed in 12 HCC tissue samples whereas the unmethylation pattern was detected in 5 HCC tissue samples. In contrast, only 2 non-HCC tissues exhibited aberrant methylation whereas the unmethylation pattern was detected in 10 non-HCC tissues: there was also a significant correlation between HCC and aberrant methylation of *SOCS-1* ($P = 0.0042$).

Neither a methylation-specific nor an unmethylation-specific band in 12 HCC and 16 non-HCC tissues was detected using the primers in the CpG island and in 5 HCC and 10 non-HCC tissue samples using the primers in the 5′-noncoding promoter region, suggesting that *SOCS-1* in these tissues was in a mosaic state of methylation. This suggestion was examined using a hepatoma cell line HLF: neither a methylation- nor an unmethylation-specific band was detected, but after 5-azacytidine treatment of the cell line for 3 days, which cancels methylation of the gene,[22] an unmethylation-specific band appeared, demonstrating that *SOCS-1* in the cell line is methylated in a mosaic fashion. Consequently, *SOCS-1* gene expression was turned on as determined by RT-PCR.

Correlation between SOCS-1 methylation and clinicopathological findings

The relationship between the methylation status of *SOCS-1* and clinicopathological findings is shown in Table 1. When the methylation status in HCC tissue samples was correlated with parameters such as the presence or absence of cirrhosis as the underlying liver disease, the histological degree of HCC, tumor sizes, vascular invasion, distant metastasis, or tumor stages, no significant association was noted.

Discussion

In the current study, we analyzed the methylation status of *SOCS-1*, a negative regulator of the JAK/STAT pathway, by the MSPCR method. Using the primers located in the CpG island in the coding region, aberrant methylation was observed in 9 of 22 (41%) HCC tissue samples, and 12 of 22 (54.5%) HCC tissue samples by the use of primers in the 5′-noncoding region. The former rate is almost compatible with the incidence in a previous report.[14] It is notable that a similar or higher rate of aberrant methylation was detected in the 5′-noncoding promoter region of *SOCS-1*. It is established that methylation in the promoter region is essential in the regulation of (silencing) the genes.[16,17] The frequent occurrence of aberrant methylation in the promoter region of *SOCS-1* further supports the notion that the downregulation of SOCS-1 expression is common in human HCC. Very recently, methylation in the promoter of SOCS-1 gene was reported in pancreatic tumors.[23]

In our MSPCR analysis, a substantial number of samples showed neither the methylated nor unmethylated pattern. The reason for this dual negativity is unclear. One possibility is a mosaic methylation pattern that may exist in the *SOCS-1*. If not all the susceptible cytosine residues are methylation, i.e., a gene is methylated in a mosaic fashion, one cannot determine the methylation status by MSPCR. This possibility was confirmed using a hepatoma cell line, as shown in the Results section. Neither a methylation- nor an unmethylation-specific band was detected, but after

5-azacytidine treatment of the cell line for 3 days, which cancels methylation of the gene,[22] an unmethylation-specific band appeared, demonstrating that *SOCS-1* in the cell line is methylated in a mosaic fashion.

SOCS-1 transcription is activated by signal transducer and activator of transcription (STAT) and the resultant proteins negatively regulate the JAK/STAT pathways either by directly inhibiting JAKs or by binding to receptors and blocking further association with STATs. Of the eight SOCS family members, SOCS-1 is a negative regulator of IL-6 signals. The silencing of *SOCS-1* results in constitutive activation of the JAK/STAT pathway. Without negative feedback by SOCS-1, the downstream pathways and target genes are strongly activated.[24] There are several lines of evidence supporting the idea that the JAK/STAT pathway may be involved in oncogenesis. The constitutive activation of the JAK/STAT pathway including STAT3 is observed in a number of transformed cells.[25] Thus, SOCS-1 is considered to be a tumor suppressor candidate, which chiefly has a role in the development of hematopoietic malignancies.[26] Also, an association of the SOCS-1 in hepatocarcinogenesis has recently been suggested.[15] There are a variety of gene products in the downstream of the JAK/STAT pathway, including c-*myc* or c-*fos*.[27] The activation of the pathway thus may cause an activation of oncogenes or growth-associated genes and eventually lead to oncogenesis. The precise role of SOCS-1 in hepatocarcinogenesis is currently unclarified and requires further study, but it might play an essential role in the majority of HCCs.

Our current results confirmed those of a previous study[14] and added a new piece of information on methylation of the promoter region of *SOCS-1*. However, the presence of cases negative for both methylation and unmethylation may limit the application of this technique for the analysis of hepatocarcinogenesis. In addition, recently the association between the core protein of hepatitis C virus and the JAK/STAT pathway has been reported as a potential proliferator of hepatocytes.[28] Besides aberrant methylation, association of SOCS-1 with HCV may cause a down-regulation of *SOCS-1* expression. In relation to this issue, it is interesting to note that a few patients in our series exhibited aberrant methylation of *SOCS-1* in the adjacent non-HCC tissue samples. Infection with HCV, which is present in all patients, may be associated with *SOCS-1* expression in human HCC tissues. Further studies are necessary for deciphering the complicated involvement of the SOCS-1 and JAK/STAT pathway in hepatocarcinogenesis, possibly in association with HCV infection.

References

1. Chen CJ, Yu MW, Liaw YF. Epidemiological characteristics and risk factors of hepatocellular carcinoma. J Gastroenterol Hepatol 1997;12:S294–308.
2. Saito I, Miyamura T, Ohbayashi A, Harada H, Katayama T, Kikuchi S, et al. Hepatitis C virus infection is associated with the development of hepatocellular carcinoma. Proc Natl Acad Sci U S A 1990;87:6547–9.
3. Robinson WS. Molecular events in the pathogenesis of hepadnavirus-associated hepatocellular carcinoma. Annu Rev Med 1994;45:297–323.
4. Umeda T, Hino O. Molecular aspects of human hepatocarcinogenesis mediated by inflammation: from hypercarcinogenic state to normo- or hypocarcinogenic state. Oncology 2002;62:38–42.
5. Kim CM, Koike K, Saito I, Miyamura T, Jay G. HBx gene of hepatitis B virus induces liver cancer in transgenic mice. Nature (Lond) 1991;351:317–20.
6. Moriya K, Fujie H, Shintani Y, Yotsuyanagi H, Tsutsumi T, Matsuura Y, et al. The core protein of hepatitis C virus induces hepatocellular carcinoma in transgenic mice. Nat Med 1998; 41065–7.
7. Lerat H, Honda M, Beard MR, Loesch K, Sun J, Yang Y, et al. Steatosis and liver cancer in transgenic mice expressing the structural and nonstructural proteins of hepatitis C virus. Gastroenterology 2002;122:352–65.
8. Koike K, Tsutsumi T, Fujie H, Shintani Y, Moriya K. Role of hepatitis viruses in hepatocarcinogenesis. Oncology 2002;62:29–37.
9. Satoh S, Daigo Y, Furukawa Y, Kato T, Miwa N, Nishiwaki T, et al. AXIN1 mutations in hepatocellular carcinomas, and growth suppression in cancer cells by virus-mediated transfer of AXIN1. Nat Genet 2000;24:245–50.
10. Fujie H, Moriya K, Shintani Y, Tsutsumi T, Takayama T, Makuuchi M, et al. Frequent β-catenin aberration in human hepatocellular carcinoma. Hepatol Res 2001;20:39–51.
11. Matsuda Y, Ichida T, Matsuzawa J, Sugimura K, Asakura H. p16(INK4) is inactivated by extensive CpG methylation in human hepatocellular carcinoma. Gastroenterology 1999;116:394–400.
12. Starr R, Willson TA, Viney EM, Murray LJ, Rayner JR, Jenkins BJ, et al. A family of cytokine-inducible inhibitors of signaling. Nature (Lond) 1997;387:917–21.
13. Endo TA, Masuhara M, Yokouchi M, Suzuki R, Sakamoto H, Mitsui K, et al. A new protein containing an SH2 domain that inhibits JAK kinases. Nature 1997;387:921–4.
14. Naka T, Matsumoto T, Narazaki M, Fujimoto M, Morita Y, Ohsawa Y, et al. Accelerated apoptosis of lymphocytes by augmented induction of Bax in SSI-1 (STAT-induced STAT inhibitor-1) deficient mice. Proc Natl Acad Sci U S A 1998;95: 15577–82.
15. Yoshikawa H, Matsubara K, Qian GS, Jackson P, Groopman JD, Manning JE, et al. SOCS-1, a negative regulator of the JAK/STAT pathway, is silenced by methylation in human hepatocellular carcinoma and shows growth-suppression activity. Nat Genet 2001;28:29–35.
16. Jaenisch R, Bird A. Epigenetic regulation of gene expression: how the genome integrates intrinsic and environmental signals. Nat Genet 2003;33:245–54.
17. Herman JG, Baylin SB. Promoter-region hypermethylation and gene silencing in human cancer. Curr Top Microbiol Immunol 2000;249:35–54.
18. Desmet VJ, Gerber M, Hoofnagle JH, Manns M, Scheuer PJ. Classification of chronic hepatitis: diagnosis, grading and staging. Hepatology 1994;19:1513–20.
19. Hermanek P, Sobin LH. UICC TNM classification of malignant tumors. 4th ed. Berlin: Splinger; 1987.
20. Yotsuyanagi H, Yasuda K, Iino S, Moriya K, Fujie H, Shintani Y, et al. Persistent viremia after recovery from self-limited acute hepatitis B. Hepatology 1998;27:1377–82.

21. Herman JG, Graff JR, Myohanen S, Nelkin BD, Baylin SB. Methylation-specific PCR: a novel PCR assay for methylation status of CpG islands. Proc Natl Acad Sci U S A 1996;93:9821–6.
22. Velicescu M, Weisenberger DJ, Gonzales FA, Tsai YC, Nguyen CT, Jones PA. Cell division is required for de novo methylation of CpG islands in bladder cancer cells. Cancer Res 2002;62:2378–84.
23. House MG, Guo M, Iacobuzio-Donahue C, Herman JG. Molecular progression of promoter methylation in intraductal papillary mucinous neoplasms (IPMN) of the pancreas. Carcinogenesis (Oxf) 2003;24:193–8.
24. Greenhalgh CJ, Miller ME, Hilton DJ, Lund PK. Suppressors of cytokine signaling: relevance to gastrointestinal function and disease. Gastroenterology 2002;123:2064–81.
25. Kishimoto T, Kikutani H. Knocking the SOCS off a tumor suppressor. Nat Genet 2001;28:4–5.
26. Rottapel R, Ilangumaran S, Neale C, La Rose J, Ho JM, Nguyen MH, et al. The tumor suppressor activity of SOCS-1. Oncogene 2002;21:4351–62.
27. Darnell JE Jr, Kerr IM, Stark GR. Jak-STAT pathways and transcriptional activation in response to IFNs and other extracellular signaling proteins. Science 1994;264:1415–21.
28. Yoshida T, Hanada T, Tokuhisa T, Kosai K, Sata M, Kohara M, et al. Activation of STAT3 by the hepatitis C virus core protein leads to cellular transformation. J Exp Med 2002;196:641–53.

GASTROENTEROLOGY 2004;126:840–848

BASIC–LIVER, PANCREAS, AND BILIARY TRACT

Hepatitis C Virus Infection and Diabetes: Direct Involvement of the Virus in the Development of Insulin Resistance

YOSHIZUMI SHINTANI,* HAJIME FUJIE,* HIDEYUKI MIYOSHI,* TAKEYA TSUTSUMI,* KAZUHISA TSUKAMOTO,† SATOSHI KIMURA,* KYOJI MORIYA,* and KAZUHIKO KOIKE*
Departments of *Internal Medicine and †Metabolic Diseases, Graduate School of Medicine, University of Tokyo, Tokyo, Japan

See editorial on page 917.

Background & Aims: Epidemiological studies have suggested a linkage between type 2 diabetes and chronic hepatitis C virus (HCV) infection. However, the presence of additional factors such as obesity, aging, or cirrhosis prevents the establishment of a definite relationship between these 2 conditions. *Methods:* A mouse model transgenic for the HCV core gene was used. *Results:* In the glucose tolerance test, plasma glucose levels were higher at all time points including in the fasting state in the core gene transgenic mice than in control mice, although the difference was not statistically significant. In contrast, the transgenic mice exhibited a marked insulin resistance as revealed by the insulin tolerance test, as well as significantly higher basal serum insulin levels. Feeding with a high-fat diet led to the development of overt diabetes in the transgenic mice but not in control mice. A high level of tumor necrosis factor-α, which has been also observed in human chronic hepatitis C patients, was considered to be one of the bases of insulin resistance in the transgenic mice, which acts by disturbing tyrosine phosphorylation of insulin receptor substrate-1. Moreover, administration of an anti-tumor necrosis factor-α antibody restored insulin sensitivity. *Conclusions:* The ability of insulin to lower the plasma glucose level in the HCV transgenic mice was impaired, as observed in chronic hepatitis C patients. These results provide a direct experimental evidence for the contribution of HCV in the development of insulin resistance in human HCV infection, which finally leads to the development of type 2 diabetes.

Approximately 200 million people are chronically infected with hepatitis C virus (HCV) in the world. Chronic HCV infection may lead to cirrhosis and hepatocellular carcinoma, thereby being a worldwide problem both in medical and socioeconomical aspects.[1,2] In addition, chronic HCV infection is a multifaceted disease, which is associated with numerous clinical manifestations, such as essential mixed cryoglobulinemia, porphyria cutanea tarda, and membranoproliferative glomerulonephritis.[3] Recent epidemiological studies have added another clinical condition, type 2 diabetes, to a spectrum of HCV-associated diseases.[4–7] However, the establishment of a definite causative relationship between HCV infection and diabetes is hampered by the presence of other factors such as obesity, aging, or liver injury in patients with chronic HCV infection.

Type 2 diabetes is a complex, multisystem disease with a pathophysiology that includes a defect in insulin secretion, increased hepatic glucose production, and resistance to the action of insulin, all of which contribute to the development of overt hyperglycemia.[8,9] Although the precise mechanisms whereby these factors interact to produce glucose intolerance and diabetes are uncertain, it has been suggested that the final common pathway responsible for the development of type 2 diabetes is the failure of the pancreatic β-cells to compensate for the insulin resistance. Hyperinsulinemia in the fasting state is observed relatively early in type 2 diabetes, but it is considered to be a secondary response that compensates for the insulin resistance.[8,9] Overt diabetes occurs over time when pancreatic β-cells bearing the burden of increased insulin secretion fail to compensate for the insulin resistance.

In this study, to elucidate the role of HCV in a possible association between diabetes and HCV infection, transgenic mice that carry the core gene of HCV[10,11] were analyzed. We found that these mice developed insulin resistance. An addition of a high-calorie diet led to the development of type 2 diabetes by dis-

Abbreviations used in this paper: EDL, extensor digitorum longus; ELISA, enzyme-linked immunosorbent assay; FPG, fasting plasma glucose; HCV, hepatitis C virus; IRS, insulin receptor substrate; JNK, c-Jun N-terminal kinase; TNF-α, tumor necrosis factor-α.

0016-5085/04/$30.00
doi:10.1053/j.gastro.2003.11.056

rupting the balance between insulin resistance and secretion.

Materials and Methods

Transgenic Mice

The production of HCV core gene transgenic mice has been described previously.[11] Briefly, the core gene from HCV of genotype 1b, which is placed downstream of a transcriptional regulatory region from the hepatitis B virus, was introduced into C57BL/6 mouse embryos (Clea Japan, Tokyo, Japan). The mice were cared for according to institutional guidelines, fed an ordinary chow diet (Funabashi Farms, Funabashi, Japan), and maintained in a specific pathogen-free state. At an indicated time, the mice were fed a high-fat diet (Oriental Yeast Co., Ltd., Tokyo, Japan) for up to 2 months. Caloric content of food was 4.70 kcal/g for high-fat diet and 3.56 kcal/g for ordinary diet. The high-fat diet contains 18.5% protein, 22.1% fat (4.7% vegetable fat and 17.4% animal fat), 5.4% ash, 2.5% fiber, 6.5% moisture, and 45.0% carbohydrate, and the ordinary diet contains 22.4% protein, 5.7% fat, 6.6% ash, 3.1% fiber, 7.7% moisture, and 54.5% carbohydrate. Because there is a sex preference in the development of liver lesion in the transgenic mice, we used only male mice that were heterozygously transgenic for the core gene, and as controls we used nontransgenic litter mates of the transgenic mice. Transgenic mice carrying the HCV envelope genes under the same regulatory region as that in the core gene transgenic mice were also used as controls.[12] At least 5 mice were used in each experiment and the data were subjected to statistical analysis.

Glucose Tolerance Test

The mice were fasted for >16 hours before the study. D-Glucose (1g/kg body weight) was administered by intraperitoneally (IP) injection to conscious mice. Blood was drawn at different time points from the orbital sinus, and plasma glucose concentrations were measured by using an automatic biochemical analyzer DRI-CHEM 3000V (Fuji Film, Tokyo, Japan). The levels of serum insulin were determined by radioimmunoassay (BIOTRAK; Amersham Pharmacia Biotech, Piscataway, NJ) with rat insulin as a standard.

Insulin Tolerance Test

The mice were fed freely and then fasted during the study period. Human insulin (1 U/kg body weight) (Humulin; Novo Nordisk, Denmark) was administered by IP injection to fasted conscious mice, and glucose concentrations were determined at the time points indicated. Values were normalized to the baseline glucose concentration at the administration of insulin.

Morphometric Analysis

Sections of the pancreas were prepared and evaluated for morphometry after H&E staining or immunostaining. Relative islet area and islet number were determined with an image analyzer (QUE-2; Olympus Optical Co., Tokyo, Japan).

Enzyme-Linked Immunosorbent Assay

ELISA for mouse tumor necrosis factor (TNF)-α was performed using a commercially available mouse TNF-α ELISA kit (BioSource International, Camarillo, CA). Samples were prepared as reported previously.[13] Briefly, the liver of transgenic and control mice were lysed with a buffer containing 1% Tween 80, 10 mmol/L Tris-HCl [pH 7.4], 1 mmol/L EDTA, 0.05% sodium azide, 2 mmol/L PMSF, and the Protease Inhibitor Cocktail (Complete; Roche Molecular Biochemicals, Indianapolis, IN) and homogenized on ice for 20 seconds. The homogenates were centrifuged at 11,000 × *g* for 10 minutes at 4° C, and the supernatants were collected and assayed. ELISA was performed in triplicate for each sample. The concentrations of the cytokines in the liver were normalized by determining the amount of total protein in each sample using the BCA Protein Assay Kit (Pierce, Rockford, IL).

Immunoprecipitation and Western Blotting

For immunoprecipitation studies, liver tissues were homogenized in lysis buffer (10 mmol/L Tris-HCl at pH 7.5, 150 mmol/L NaCl, 10 mmol/L sodium pyrophosphate, 1.0 mmol/L β-glycerophosphate, 1.0 mmol/L sodium orthovanadate [Na_3VO_4], 50 mmol/L sodium fluoride [NaF], the Protease Inhibitor Cocktail [Complete, Roche Molecular Biochemicals], and 1.0% Triton X-100), and homogenates were precipitated with an anti–insulin receptor substrate (IRS)-1 or anti–IRS-2 rabbit polyclonal antibody (UBI, Lake Placid, NY) and then with Sepharose 4B beads (Amersham Biosciences). Resulting pellets were washed 3 times and then subjected to Western blotting. Pellets were resuspended in Western sample buffer (5% β-mercaptoethanol, 2% sodium dodecyl sulfate, 62.5 mmol/L Tris-HCl, 1 mmol/L EDTA, 10% glycerol), and then subjected to 2%–15% gradient sodium dodecyl sulfate/PAGE (PAG Mini "DAIICHI" 2/15 (13W), Daiichi Diagnostics, Tokyo, Japan), and electrotransferred to polyvinylidene difluoride membranes (Immobilon-P, Millipore, Bedford, MA). The filter was then reacted with antiphosphorylated tyrosine (Santa Cruz Biotechnology Inc., Santa Cruz, CA), antiphosphorylated serine (Cell Signaling Technology, Inc., Beverly, MA), anti–IRS-1 or anti–IRS-2 mouse monoclonal antibody (BD Biosciences, Lexington, KY), followed by immunostaining with secondary biotinylated IgG (Vector Labs, Inc., Burlingame, CA) and visualization using an ECL kit (Amersham Intl., Buckinghamshire, UK).[14]

Hyperinsulinemic-Euglycemic Clamp

Mice underwent a hyperinsulinemic-euglycemic clamp using D-[3-^{3}H]glucose (NEN Life Science, Boston, MA) to measure the rate of glucose appearance and hepatic glucose production (HGP) as described previously.[15] Three days after jugular catheter placement, a hyperinsulinemic-euglycemic clamp was conducted with a continuous infusion of human

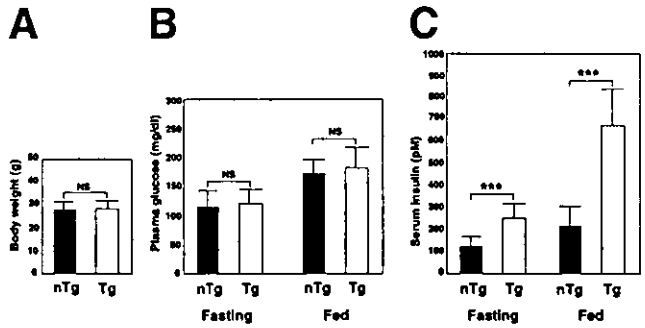

Figure 1. Altered glucose homeostasis in hepatitis C virus core gene transgenic mice. (*A*) Body weight of 2-month-old mice (n = 10 in each group). (*B*) Plasma glucose levels in fasting or fed mice (n = 10 in each group). (*C*) Serum insulin levels in fasting or fed mice (n = 10 in each group). The insulin level was significantly higher in the core gene transgenic mice than in control mice. Values are mean ± standard error; ***$P < 0.001$; NS, statistically not significant; nTg, nontransgenic mice; Tg, transgenic mice.

insulin to raise serum insulin within a physiological range. Blood samples were drawn at intervals for the immediate measurement of blood glucose concentration, and 20% glucose was infused at variable rates to maintain blood glucose at ca. 125 mg/dL. All infusions were done using microdialysis pumps (KD Scientific Inc., Boston, MA). The rate of glucose appearance (mg/kg per minute), which equals the rate of total body glucose utilization during steady state, was calculated as the ratio of the rate of infusion of [3-^{3}H]glucose and the steady state plasma [^{3}H-]glucose specific activity. HGP (mg/kg/min) during clamps was determined by subtracting the glucose infusion rate from the rate of glucose appearance.

Glucose Uptake by Skeletal Muscle

The extensor digitorum longus (EDL) or soleus muscle was excised from 2-month-old mice and exposed to insulin at the indicated concentrations. 2-Deoxyglucose uptake was determined as described previously.[16]

Treatment With Anti-TNF-α Antibody

To suppress TNF-α, a dose of 200 μg/mouse of neutralizing hamster monoclonal antibody (TN3-19.12, Santa Cruz Biotechnology Inc.) was administered by IP injection on days 1 and 4, and plasma glucose and insulin levels were determined at day 5.[17]

Statistical Analysis

The results are expressed as means ± standard error. The significance of the difference in means was determined by Student *t* test or Mann–Whitney *U* test whenever appropriate. $P < 0.05$ was considered significant.

Results

Hyperinsulinemia and Insulin Resistance in Transgenic Mice

At the age between 1 and 12 months, there was no significant difference in body weight between the core gene transgenic mice and control mice. Figure 1*A* shows body weight of 2-month-old mice. Fasting plasma glucose (FPG) levels were slightly elevated in the core gene transgenic mice compared with control mice, but the difference was not significant ($P = 0.79$, Figure 1*B*). In contrast, there was a marked increase in the level of serum insulin in the core gene transgenic mice than control mice ($P < 0.001$, Figure 1*C*). Hyperinsulinemia was observed in the core gene transgenic mice as early as 1 month old. These findings suggest that decreased responsiveness to the hormone may have resulted in compensatory hyperinsulinemia. Administration of glucose to 2-month-old core gene transgenic mice revealed mild glucose intolerance compared with control mice of the same age, but the difference was not statistically significant at any time points measured (Figure 2*A*). HCV envelope gene transgenic mice of the same age, in which the envelope genes were expressed under the same transcriptional regulatory region as the core gene transgenic mice, did not manifest hyperinsulinemia or elevated FPG levels, indicating that not the transcriptional regulatory region used but the expressed gene itself is essential in this phenotype.

The insulin tolerance test conducted at the age of 2 months revealed that the reduction in plasma glucose concentration after IP insulin injection was impaired in the core gene transgenic mice, displaying higher plasma glucose levels than those in control mice at all time points measured (Figure 2*B*). At 40 and 60 minutes, the difference was statistically significant between transgenic

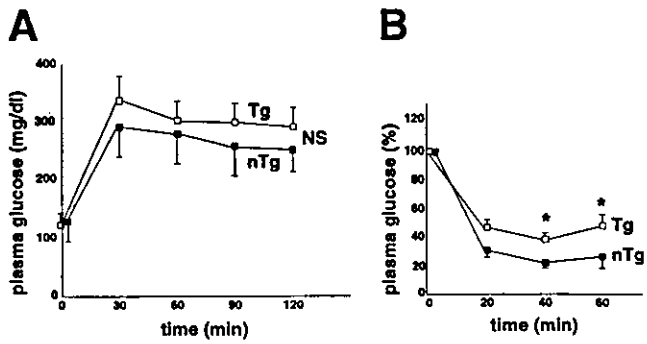

Figure 2. Insulin resistance in the core gene transgenic mice. (*A*) Glucose tolerance test (n = 5 in each group). Animals were fasted overnight (>16 hours). D-Glucose (1 g/kg body weight) was administered by IP injection to conscious mice, and plasma glucose levels were determined at the time points indicated. (*B*) Insulin tolerance test (n = 5 in each group). Human insulin (1 U/kg body weight) was administered by IP injection to fasted conscious mice and glucose concentrations were determined. Values were normalized to the baseline glucose concentration at the time of insulin administration. Values are mean ± standard error; *$P < 0.05$; NS, statistically not significant; nTg, nontransgenic mice; Tg, transgenic mice.

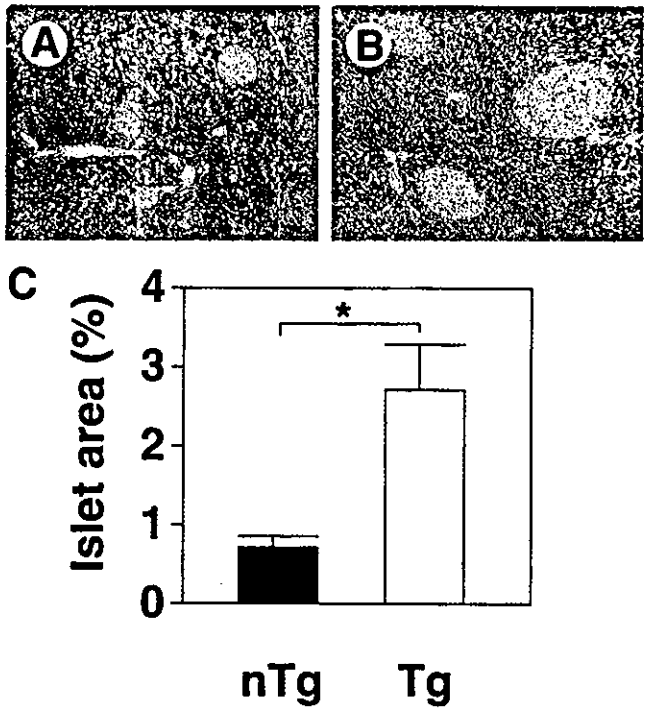

Figure 3. Analysis of pancreatic islet mass in the core gene transgenic and control mice. (*A* and *B*) Morphology of representative islets (H&E staining) from normal control mice (*A*) or the core gene transgenic mice (*B*). (*C*) Relative islet area, expressed as a percentage of the total stained pancreatic section, for control mice (nTg) and the core gene transgenic mice (Tg) (n = 10 in each group). Values are mean ± standard error; $*P < 0.05$.

and control mice (39.6 ± 1.3 vs. 24.4 ± 1.1 and 43.7 ± 2.1 vs. 26.4 ± 2.3, $P < 0.05$). These data are consistent with a defect in the actions of insulin on glucose disposal and/or production in the core gene transgenic mice.

Morphology of Pancreatic Islet Cells

Because a critical factor contributing to whether insulin resistance progresses to diabetes is the capacity of the pancreatic β-cells to respond to increased demands for insulin secretion, we evaluated the morphology of pancreatic islet cells by histologic examination. In the pancreas of HCV core gene transgenic mice, an approximately 3-fold increase in islet mass was observed (Figure 3, $P < 0.05$), which is consistent with β-cell compensation to insulin resistance. There was no infiltration of inflammatory cells within or surrounding the islets.

Feeding Transgenic Mice a High-Fat Diet Leads to Overt Diabetes

Thus, an insulin resistance is present but no apparent glucose intolerance (overt diabetes) in the HCV core gene transgenic mice. This is probably because of the genetic background of C57BL/6 mice, which has been shown to maintain either normal or mildly elevated glucose levels despite insulin resistance.[18] To determine whether a high-fat diet exacerbates the prediabetic phenotype, 2-month-old HCV core gene transgenic mice were fed a high-fat diet for up to 8 weeks. Both the transgenic and control mice showed a similar increase (about 30%) in body weight (Figure 4*A*). After 8 weeks on this diet, 100% (10 out of 10) of the transgenic mice exhibited casual (fed) plasma glucose levels >250 mg/dL, whereas none of the 10 control mice fed the same diet exhibited levels >250 mg/dL (325.0 ± 66.6 vs. 179.0 ± 17.4 mg/dL, $P < 0.01$, Figure 4*B*). Insulin levels were significantly higher in the core gene transgenic mice than in control mice both at fasting and fed state (Figure 4*C*, $P < 0.01$ and $P < 0.001$). In control mice, serum insulin levels in high-fat diet state were significantly higher than those in normal diet state at fed state (Figures 1*C* and 4*C*, $P < 0.01$). Although FPG levels were not significantly different between the transgenic and control mice, these results indicate that feeding a high-fat diet leads to the development of overt diabetes in a mouse model for HCV infection. Body weight gain, particularly with high levels of lipid, may trigger the process leading to overt diabetes in an insulin resistance model mouse with compensatory hyperplasia of islet cells.

Insulin Resistance in the Core Gene Transgenic Mice Is Chiefly Caused by Hepatic Insulin Resistance

We then investigated the mechanism of insulin resistance in the core gene transgenic mice. There was no

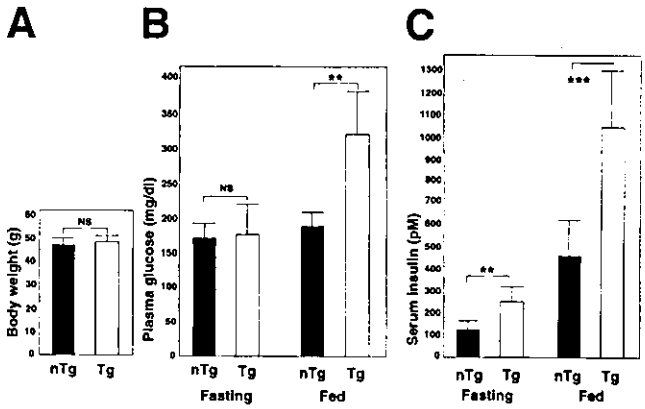

Figure 4. Body weight and glucose homeostasis after a high-fat diet. Control and transgenic mice were fed a high-fat diet for 8 weeks; thereafter, body weight and blood parameters were determined. (*A*) Body weight at the end of the high-fat diet (n = 10 in each group). (*B*) Plasma glucose levels determined in a fasting or fed state (n = 10 in each group). (*C*) Serum insulin levels in a fasting or fed state (n = 10 in each group). Values are mean ± standard error; NS, statistically not significant; $**P < 0.01$; $***P < 0.001$; nTg, nontransgenic mice; Tg, transgenic mice.

significant difference in body weight between the transgenic and control mice as already shown in Figure 1*A*. After the age of 3 months, the core gene transgenic mice developed hepatic steatosis, which is known to be one of the causes of insulin resistance in humans.[19] However, in 1-month-old mouse livers that were used in the analysis of insulin resistance, no hepatic steatosis was noted. No difference was observed in the levels of free fatty acids in the sera between the transgenic and control mice (0.56 ± 0.33 vs. 0.50 ± 0.21 mmol/L, n = 7 in each group, P = 0.65).

Then, we explored the role of the liver in pathogenesis of insulin resistance in the core gene transgenic mice. To directly measure HGP, the hyperinsulinemic-euglycemic clamp technique was conducted as described in Materials and Methods. The core gene transgenic mice showed a normal or slightly lower rate of HGP during the basal period as compared with control mice (Figure 5*A*). Although insulin infusion during the clamp suppressed HGP by 60% in the control mice, insulin induced little effect on HGP of the core gene mice (Figure 5*A*). This is consistent with the notion that insulin resistance in the core gene transgenic mice is chiefly depending on the shortage of insulin action on the liver.

To study the involvement of muscles in the development of insulin resistance in the core gene transgenic mice, we then examined whether or not insulin-stimulated glucose uptake is impaired in the skeletal muscles. The extensor digitorum longus muscle (EDL) from 2-month-old core gene transgenic and control mice were excised and exposed to insulin at the intermediate (0.30 nmol/L) and maximal (10.0 nmol/L) concentrations. There was no significant difference in 2-deoxyglucose uptake in the EDL muscle between the core gene transgenic mice and control mice at either insulin concentration (Figure 5*B*, at 0.30 nmol/L, P = 0.23 and at 10.0 nmol/L, P = 0.76). As another representative muscle that differs from EDL in metabolic properties, the soleus muscle was examined in the same manner as EDL. 2-Deoxyglucose uptake by the soleus muscle was not significantly different between the core gene transgenic and control mice (Figure 5*C*, at 0.30 nmol/L, P = 0.49 and at 10.0 nmol/L, P = 0.49). Thus, in the core gene transgenic mice, contribution of the peripheral skeletal muscle in the development of insulin resistance is negligible. This is in agreement with the observation that the core protein was exclusively present in the liver as detected by Western blotting,[20] which was confirmed by a sensitive enzyme immunoassay (Tsutsumi T. et al., unpublished data, December 2002).[21]

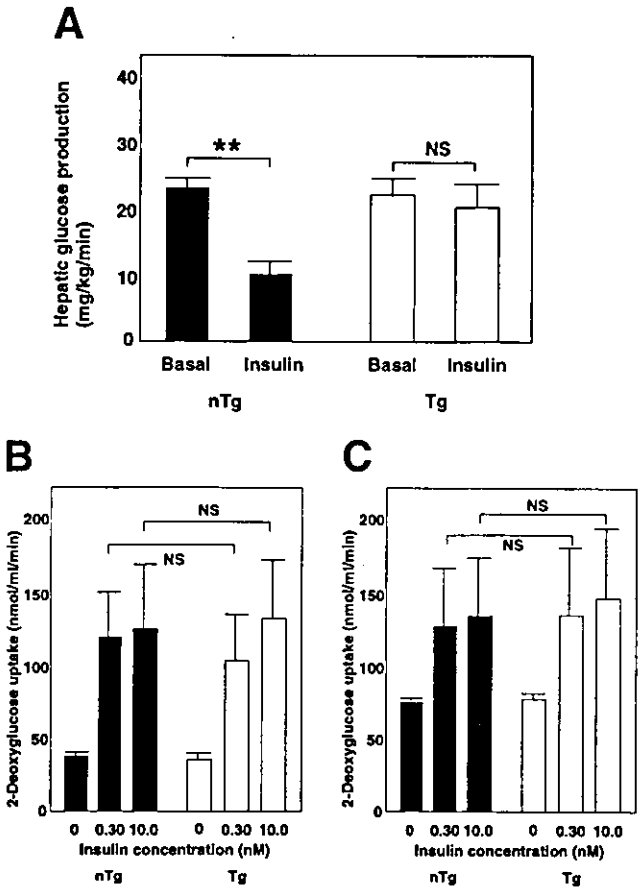

Figure 5. Characterization of glucose metabolism in the core gene transgenic mice. (*A*) Hyperinsulinemic-euglycemic clamp. Hepatic glucose production was calculated using hyperinsulinemic-euglycemic clamp. There was a failure of insulin to suppress hepatic glucose production in the core gene transgenic mice (n = 5 in each group). (*B* and *C*) Glucose uptake by the muscle after insulin stimulation. The extensor digitorum longus muscle (*A*) or soleus muscle (*B*) of 2-month-old mice were excised and exposed to insulin at intermediate (0.30 nmol/L) and maximal (10.0 nmol/L) concentrations. 2-Deoxyglucose uptake was determined as described in the Materials and Methods section (n = 8 in each group). Values are mean ± standard error; NS, statistically not significant; nTg, nontransgenic mice; Tg, transgenic mice.

Elevated TNF-α Level and Altered Tyrosine Phosphorylation of Insulin Receptor Substrate-1 in the Liver and Insulin Resistance

We have noted an increase in TNF-α levels in the liver of HCV core gene transgenic mice,[13] which has also been documented in the sera of human hepatitis C patients.[22–25] On the other hand, TNF-α has been shown to induce insulin resistance in experimental animals and cultured cells.[26–29] Therefore, we next determined the protein expression level of TNF-α by ELISA in the liver of these mice that were used in the current study. The TNF-α levels in the liver of 2-month-old transgenic mice were 702.2 ± 283.3 pg/mg protein and 313.5 ±

113.6 pg/mg protein in that of 2-month-old control mice (n = 10 in each group, $P < 0.001$). Thus, the levels of TNF-α exhibited a more than 2-fold increase in the HCV core gene transgenic mice compared with the control mice, which may be associated with insulin resistance.

Suppression of tyrosine phosphorylation of IRS-1 and -2 is one of the mechanisms by which a high level of TNF-α causes insulin resistance.[29-31] We, therefore, examined the suppression of tyrosine phosphorylation of IRS-1 in response to insulin action in the core gene transgenic mice. Twenty minutes after the administration of human insulin (1 U/kg body weight), when the plasma glucose levels decreased (Figure 2*B*), IRS-1 in the liver of control mice exhibited a marked phosphorylation of its tyrosine. In contrast, phosphorylation level of tyrosine in IRS-1 in the liver of core gene transgenic mice manifested apparently no increase compared with the basal level after the administration of insulin (Figure 6). In contrast, there was no difference in the time course of tyrosine phosphorylation of IRS-2 between the core gene transgenic and control mice (data not shown). These results indicate that a suppression of tyrosine phosphorylation of IRS-1, that is, a suppression of the insulin action in the liver, is at least one of the mechanisms of insulin resistance in HCV transgenic mice, whereas pathways other than IRS-1 may also be involved.

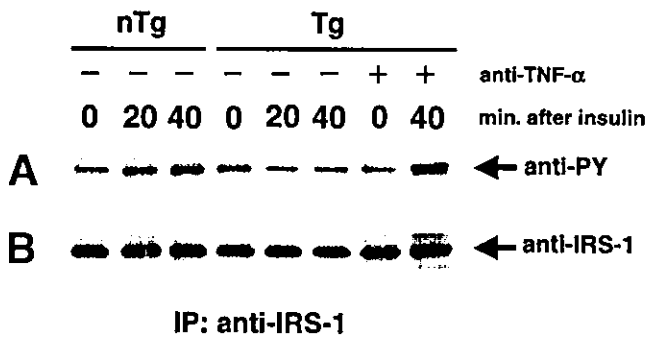

Figure 6. Phosphorylation of tyrosine in IRS-1 in response to insulin stimulation. Liver tissues from control mice and core gene transgenic mice with or without anti-TNF-α antibody treatment were analyzed before and 20 and 40 minutes after insulin administration. The samples were subjected to immunoprecipitation with anti-IRS-1 antibody and subsequently immunoblotted with antibodies as indicated. Experiments were performed in triplicate, and a representative picture is shown. (*A*) Immunoblot with antiphosphotyrosine antibody. There was no augmentation of phosphorylation of tyrosine in IRS-1 after insulin stimulation in the core gene transgenic mice, whereas tyrosine phosphorylation was markedly enhanced in control mice. Insulin-stimulated tyrosine phosphorylation was restored 40 minutes after anti-TNF-α antibody treatment. (*B*) Immunoblotting with anti-IRS-1 antibody as a control of IRS-1 load. nTg, nontransgenic mice; Tg, transgenic mice; anti-PY, antiphosphotyrosine antibody; anti-PS, antiphosphoserine antibody. IP, immunoprecipitation.

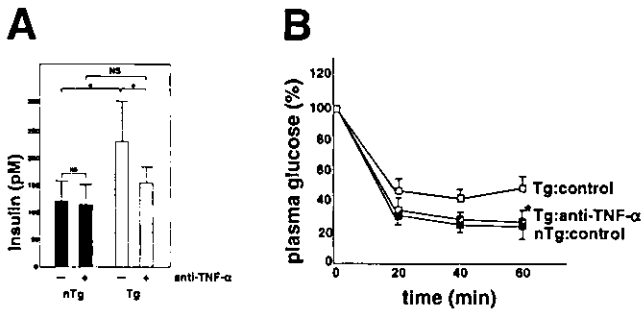

Figure 7. Serum insulin levels and insulin tolerance test after anti-TNF-α antibody treatment. (*A*) Serum insulin levels were determined in the fasting state with or without anti-TNF-α antibody treatment as described in the Materials and Methods section. Insulin levels decreased significantly after anti-TNF-α antibody treatment in the core gene transgenic mice (n = 5 in each group). (*B*) Insulin tolerance test (n = 5 in each group). Human insulin was administered by IP injection to fasted conscious mice and glucose concentrations were determined 24 hours after the second administration of anti-TNF-α antibody. As control, mice were injected with hamster IgG instead of anti-TNF-α antibody. Values were normalized to the baseline glucose concentration at the time of insulin administration. Values are mean ± standard error; $*P < 0.05$ when compared with Tg control; nTg, nontransgenic mice; Tg, transgenic mice.

The c-Jun N-terminal kinase (JNK) pathway has been shown to mediate the inhibitory effect of TNF-α on insulin action through the phosphorylation of serine in IRS-1.[32,33] Because an activation of the JNK pathway was observed in the liver of core gene transgenic mice,[13] phosphorylation of serine residues in IRS-1 was examined using antiphosphorylated serine monoclonal antibodies (Ser^{307} and Ser^{612}). However, there was no difference in the time course of serine phosphorylation after insulin stimulation between the core gene transgenic and control mice (data not shown).

Blockade of TNF-α Action Restores Insulin Sensitivity

Then the anti-TNF-α antibody was administered to block the in vivo activity of TNF-α in mice as described in the Materials and Methods section.[17] Twenty-four hours after the second administration of the anti-TNF-α antibody (200 μg/mouse), serum insulin levels in transgenic mice became significantly lower than the baseline (Figure 7*A*, 230.8 ± 70.7 vs. 153.6 ± 17.4 pmol/L, $P < 0.05$). Serum insulin levels in control mice also decreased, but there was no significant difference from the baseline (123.3 ± 36.1 vs. 112.0 ± 39.7 pmol/L, $P = 0.25$). Levels of FPG also decreased, but the difference from the baseline was not statistically significant. The insulin tolerance test conducted 24 hours after the second administration of anti-TNF-α antibody is shown in Figure 7*B*. As expected from serum insulin levels, anti-TNF-α antibody treatment restored the sen-

sitivity of the core gene transgenic mice to insulin activity. At this time point, phosphorylation of tyrosine in IRS-1 in the liver of transgenic mice in response to insulin action was restored to a similar level to that in control mice (Figure 6*A*, 40 minutes after insulin administration). These results strongly support the notion that the increased level of TNF-α is one of the bases for insulin resistance in the HCV core gene transgenic mice.

Taken together, these data indicate that the presence of the HCV core protein in the liver, at a level similar to that in human chronic hepatitis C patients,[21] confers insulin resistance to the mice by affecting the liver, by disturbing the insulin-induced suppression of hepatic glucose production.[34,35]

Discussion

Since Allison et al.[4] reported an association between HCV infection and diabetes, evidence has been accumulating connecting these 2 conditions. In such studies, HCV infection has a significantly stronger association with diabetes than hepatitis B viral infection.[4–7] The variables other than HCV infection that are associated with diabetes are cirrhosis, male sex,[5] and aging.[6] In addition to these clinic-based, case-control studies, Mehta et al.[7] have reported the result of investigation at population level. In this cross-sectional national survey, persons 40 years or older with HCV infection were more than 3 times more likely to have type 2 diabetes than those without HCV infection. Thus, the association of HCV infection with diabetes has become closer as shown by epidemiological studies. However, there are some difficulties in establishing a definite relationship between HCV infection and diabetes on the basis of epidemiological studies; in patients, there are other numerous factors perturbing the verification of the definite relationship, such as obesity, aging, or particularly advanced liver injuries. Moreover, the biological mechanism underlying diabetes or insulin resistance in HCV infection is unknown. In vitro or cultured cell studies have a very limited utility for the study of insulin resistance or diabetes because insulin resistance is a condition that involves multiple organs, such as the skeletal muscles and liver. Thus, the use of good experimental animal model systems may be useful both in establishing a definite relationship between diabetes and HCV infection and in elucidating the role of HCV in the development of insulin resistance.

In the current study, the HCV core gene transgenic mice exhibited insulin resistance as early as 1-month old, despite an apparent absence of glucose intolerance. Development of insulin resistance without any liver injury[10,11] or excessive body weight gain, as shown in the current study, clearly indicates that infection of HCV per se is a cause of the development of insulin resistance. Although only the core protein is expressed in these mice instead of HCV replication in humans, the fact that the intrahepatic core protein levels are similar between the core gene transgenic mice and chronic hepatitis C patients[20] warrants extrapolating the result into hepatitis C patients. Certainly, dispersion in the intrahepatic core protein levels in human chronic hepatitis C patients compared with the constant amount of the core protein must be taken into account. The occurrence of insulin resistance in the core gene transgenic mice as early as 1-month old also excluded the possibility that aging is a cause of insulin resistance. Nonetheless, aging could be an aggravating factor for insulin resistance. Thus, the current analysis shows a definite causal relationship between HCV infection and the development of insulin resistance.

Our earlier studies have shown the development of hepatic steatosis in these HCV core gene transgenic mice after the age of 3 months.[11] However, insulin resistance invariably preceded the occurrence of hepatic steatosis, indicating that insulin resistance is not a consequence of hepatic steatosis in these mice. Certainly, it is possible that insulin resistance in the core gene transgenic mice may be affected or aggravated after the occurrence of hepatic steatosis. On the other hand, insulin resistance may be one of the factors that cause hepatic steatosis,[19] whereas the impairment of very-low-density lipoprotein (VLDL) secretion from the liver and hypo-β-oxidation of fatty acids are considered to be the bases of development of hepatic steatosis in the core gene transgenic mice.[21,36]

The general mechanism underlying insulin resistance is not precisely understood and is considered to be multifactorial.[8,9,37,38] Chiefly, it involves glucose consumption by the skeletal muscle and glucose production in the liver. Our current analysis revealed a failure of insulin in the suppression of HPG in the liver and an absence of suppression of glucose uptake by the muscles in the core gene transgenic mice. Combined, these results indicate the insulin resistance in the core gene transgenic mice is chiefly due to hepatic insulin resistance. An elevated intrahepatic TNF-α level plays one of the roles in causing insulin resistance through suppressing insulin-induced tyrosine phosphorylation of IRS-1. It should be noted that TNF-α levels are invariably elevated in the sera of patients with HCV infection.[22] Moreover, restoration of insulin sensitivity after anti–TNF-α antibody administration strongly supports the notion that TNF-α

is, at least in this animal model, a major factor for the development of insulin resistance in HCV infection. Taken together, insulin resistance in the core gene transgenic mice mainly depends on suppression of the inhibitory effect of insulin on hepatic glucose production. This is consistent with the observation that the core protein is present only in the liver but absent in the skeletal muscle of the core gene transgenic mice (Tsutsumi T., unpublished data, December 2002).[21] Impairment in other undetermined pathways may also be responsible for the development of insulin resistance in HCV infection.

Insulin resistance alone does not always lead to the development of overt diabetes in humans or murine models. Particularly, in the models with the C57/BL6 strain,[18] hyperplasia of the islets of Langerhans in the pancreas compensates for insulin resistance by secreting higher amounts of insulin. Along with a gain in body weight by being fed a high-calorie diet, the core gene transgenic mice but no control mice developed overt diabetes, showing that obesity is a risk factor for diabetes as observed in patients or as shown in animal models for diabetes unrelated to HCV infection.[37,38] This observation would suggest that HCV infection confers insulin resistance and additional factors such as obesity, aging, or possibly inflammation may contribute to the complete development of overt diabetes. The effect of high-fat diet on control C57BL/6 mice may be milder in the current study compared with a previous study.[39] However, there was a substantial increase in FPG levels in high-fat-diet-fed control mice compared with normal-diet-fed control mice (Figures 1*B* and 4*B*). In addition, at fed-state, serum insulin levels in high-fat-diet-fed control mice were significantly increased compared with those in normal-diet-fed control mice (Figures 1*B* and 4*B*). It is unclear why plasma glucose levels were not very high at fed-state in control mice, but one possible explanation is the lower calorie content in the current study than those in the previous report: 4.70 kcal/g for our high-fat diet vs. 5.55 kcal/g for high-calorie diet in the previous study. A shorter duration of high-fat diet than the previous study (2 months vs. 6 months) may be another possible explanation.[39] Such a mild elevation in plasma glucose levels in high-fat-diet-fed C57BL/6 mice as the one observed in our study has also been described in previous studies.[40]

In conclusion, the HCV core protein induces insulin resistance in transgenic mice without gain in body weight at young age. These results indicate a direct involvement of HCV per se in the pathogenesis of diabetes in patients with HCV infection and provide a molecular basis for insulin resistance in such a condition.

References

1. Saito I, Miyamura T, Ohbayashi A, Harada H, Katayama T, Kikuchi S, Watanabe Y, Koi S, Onji M, Ohta Y, Choo Q, Houghton M, Kuo G. Hepatitis C virus infection is associated with the development of hepatocellular carcinoma. Proc Natl Acad Sci U S A 1990;87: 6547–6549.
2. Simonetti RG, Camma C, Fiorello F, Cottone M, Rapicetta M, Marino L, Fiorentino G, Craxi A, Ciccaglione A, Giuseppetti R, Stroffolini T, Pagliaro L. Hepatitis C virus infection as a risk factor for hepatocellular carcinoma in patients with cirrhosis. Ann Intern Med 1992;116:97–102.
3. Gumber SC, Chopra S. Hepatitis C: a multifaceted disease. Ann Intern Med 1995;123:615–620.
4. Allison ME, Wreghitt T, Palmer CR, Alexander GJ. Evidence for a link between hepatitis C virus infection and diabetes mellitus in a cirrhotic population. J Hepatol 1994;21:1135–1139.
5. Caronia S, Taylor K, Pagliaro L, Carr C, Palazzo U, Petrik J, O'Rahilly S, Shore S, Tom BD, Alexander GJ. Further evidence for an association between non-insulin-dependent diabetes mellitus and chronic hepatitis C virus infection. Hepatology 1999;30: 1059–1063.
6. Mason AL, Lau JY, Hoang N, Qian K, Alexander GJ, Xu L, Guo L, Jacob S, Regenstein FG, Zimmerman R, Everhart JE, Wasserfall C, Maclaren NK, Perrillo RP. Association of diabetes mellitus and chronic hepatitis C virus infection. Hepatology 1999;29:328–333.
7. Mehta SH, Brancati FL, Sulkowski MS, Strathdee SA, Szklo M, Thomas DL. Prevalence of type 2 diabetes mellitus among persons with hepatitis C virus infection in the United States. Ann Intern Med 2000;133:592–599.
8. Kahn BB. Type 2 diabetes: when insulin secretion fails to compensate for insulin resistance. Cell 1998;92:593–596.
9. Cavaghan MK, Ehrmann DA, Polonsky KS. Interactions between insulin resistance and insulin secretion in the development of glucose intolerance. J Clin Invest 2000;106:329–333.
10. Moriya K, Fujie H, Shintani Y, Yotsuyanagi H, Tsutsumi T, Matsuura Y, Kimura S, Miyamura T, Koike K. Hepatitis C virus core protein induces hepatocellular carcinoma in transgenic mice. Nat Med 1998;4:1065–1068.
11. Moriya K, Yotsuyanagi H, Shintani Y, Fujie H, Ishibashi K, Matsuura Y, Miyamura T, Koike K. Hepatitis C virus core protein induces hepatic steatosis in transgenic mice. J Gen Virol 1997; 78:1527–1531.
12. Koike K, Moriya K, Yotsuyanagi H, Shintani Y, Fujie H, Ishibashi K, Matsuura Y, Kurokawa K, Miyamura T. Sialadenitis resembling Sjögren's syndrome in mice transgenic for hepatitis C virus envelope genes. Proc Natl Acad Sci U S A 1997;94:233–236.
13. Tsutsumi T, Suzuki T, Moriya K, Yotsuyanagi H, Shintani Y, Fujie H, Matsuura Y, Kimura S, Koike K, Miyamura T. Intrahepatic cytokine expression and AP-1 activation in mice transgenic for hepatitis C virus core protein. Virology 2002;304:415–424.
14. Fujie H, Moriya K, Shintani Y, Tsutsumi T, Takayama T, Makuuchi M, Kimura S, Koike K. Frequent β-catenin aberration in human hepatocellular carcinoma. Hepatol Res 2001;20:39–51.
15. Ren JM, Marshall BA, Mueckler MM, McCaleb M, Amatruda JM, Shulman GI. Overexpression of Glut4 protein in muscle increases basal and insulin-stimulated whole body glucose disposal in conscious mice. J Clin Invest 1995;95:429–432.
16. Brozinick T Jr, Birnbaum MJ. Insulin, but not contraction, activates Akt/PKB in isolated rat skeletal muscle. J Biol Chem 1998;273:14679–14682.
17. Williams RO, Marinova-Mutafchieva L, Feldmann M, Maini RN. Evaluation of TNF-alpha and IL-1 blockade in collagen-induced arthritis and comparison with combined anti-TNF-alpha/anti-CD4 therapy. J Immunol 2000;165:7240–7245.
18. Polonsky KS, Sturis J, Bell GI. Seminars in medicine of the Beth

Israel Hospital, Boston. Non-insulin-dependent diabetes mellitus—a genetically programmed failure of the beta cell to compensate for insulin resistance. N Engl J Med 1996;334:777–783.
19. Chatila R, West AB. Hepatomegaly and abnormal liver tests due to glycogenosis in adults with diabetes. Medicine (Baltimore) 1996;75:327–333.
20. Koike K, Moriya K, Ishibashi K, Matsuura Y, Suzuki T, Saito I, Iino S, Kurokawa K, Miyamura T. Expression of hepatitis C virus envelope proteins in transgenic mice. J Gen Virol 1995;76:3031–3038.
21. Koike K, Tsutsumi T, Fujie H, Shintani Y, Moriya K. Role of hepatitis viruses in hepatocarcinogenesis. Oncology 2002;62: 29–37.
22. Polyak SJ, Khabar KS, Rezeiq M, Gretch DR. Elevated levels of interleukin-8 in serum are associated with hepatitis C virus infection and resistance to interferon therapy. J Virol 2001;75:6209–6211.
23. Kallinowski B, Haseroth K, Marinos G, Hanck C, Stremmel W, Theilmann L, Singer MV, Rossol S. Induction of tumour necrosis factor (TNF) receptor type p55 and p75 in patients with chronic hepatitis C virus (HCV) infection. Clin Exp Immunol 1998;111: 269–277.
24. Nelson DR, Lim HL, Marousis CG, Fang JW, Davis GL, Shen L, Urdea MS, Kolberg JA, Lau JY. Activation of tumor necrosis factor-alpha system in chronic hepatitis C virus infection. Dig Dis Sci 1997;42:2487–2494.
25. Gershon AS, Margulies M, Gorczynski RM, Heathcote EJ. Serum cytokine values and fatigue in chronic hepatitis C infection. J Viral Hepat 2000;7:397–402.
26. Moller DE. Potential role of TNF-alpha in the pathogenesis of insulin resistance and type 2 diabetes. Trends Endocrinol Metab 2000;11:212–217.
27. Halse R, Pearson SL, McCormack JG, Yeaman SJ, Taylor R. Effects of tumor necrosis factor-alpha on insulin action in cultured human muscle cells. Diabetes 2001;50:1102–1109.
28. Mishima Y, Kuyama A, Tada A, Takahashi K, Ishioka T, Kibata M. Relationship between serum tumor necrosis factor-alpha and insulin resistance in obese men with type 2 diabetes mellitus. Diabetes Res Clin Pract 2001;52:119–123.
29. Uysal KT, Wiesbrock SM, Marino MW, Hotamisligil GS. Protection from obesity-induced insulin resistance in mice lacking TNF-alpha function. Nature 1997;389:610–614.
30. Hotamisligil GS. The role of TNF alpha and TNF receptors in obesity and insulin resistance. J Intern Med 1999;245:621–625.
31. Ozes ON, Akca H, Mayo LD, Gustin JA, Maehama T, Dizon JE, Donner DB. A phosphatidylinositol 3-kinase/Akt/mTOR pathway mediates and PTEN antagonizes tumor necrosis factor inhibition of insulin signaling through insulin receptor substrate-1. Proc Natl Acad Sci U S A 2001;98:4640–4645.
32. Aguirre V, Uchida T, Yenush L, Davis R, White MF. The c-Jun NH(2)-terminal kinase promotes insulin resistance during association with insulin receptor substrate-1 and phosphorylation of Ser(307). J Biol Chem 2000;275:9047–9054.
33. De Fea K, Roth RA. Protein kinase C modulation of insulin receptor substrate-1 tyrosine phosphorylation requires serine 612. Biochemistry 1997;36:12939–12947.
34. Michael MD, Kulkarni RN, Postic C, Previs SF, Shulman GI, Magnuson MA, Kahn CR. Loss of insulin signaling in hepatocytes leads to severe insulin resistance and progressive hepatic dysfunction. Mol Cell 2000;6:87–97.
35. Cho H, Mu J, Kim JK, Thorvaldsen JL, Chu Q, Crenshaw EB 3rd, Kaestner KH, Bartolomei MS, Shulman GI, Birnbaum MJ. Insulin resistance and a diabetes mellitus-like syndrome in mice lacking the protein kinase Akt2 (PKB beta). Science 2001;292:1728–1731.
36. Perlemuter G, Sabile A, Letteron P, Topilco Samson-Bouna M-E, Chretien Y, Pessayre D, Koike K, Chapman J, Barba G, Brechot C. Hepatitis C virus core protein inhibits microsomal triglyceride transfer protein activity and very low density lipoprotein secretion: a model of viral-related steatosis. FASEB J 2002;16:185–194.
37. Kahn BB, Flier JS. Obesity and insulin resistance. J Clin Invest 2000;206:473–481.
38. Kadowaki T. Insight into insulin resistance and type 2 diabetes from knockout mouse models. J Clin Invest 2000;206:459–465.
39. Surwit RS, Feinglos MN, Rodin J, Sutherland A, Petro AE, Opara EC, Kuhn CM, Rebuffe-Scrive M. Differential effects of fat and sucrose on the development of obesity and diabetes in C57BL/6J and A/J mice. Metabolism 1995;44:645–651.
40. Devedjian JC, George M, Casellas A, Pujol A, Visa J, Pelegrin M, Gros L, Bosch F. Transgenic mice overexpressing insulin-like growth factor-II in beta cells develop type 2 diabetes. J Clin Invest 2000;105:731–740.

Received May 30, 2003. Accepted November 20, 2003.

Address requests for reprints to: Kazuhiko Koike, M.D., Department of Infectious Diseases, Internal Medicine, Graduate School of Medicine, University of Tokyo, 7-3-1 Hongo, Bunkyo-ku, Tokyo 113-8655, Japan. e-mail: kkoike-tky@umin.ac.jp; fax: (81) 3-5800-8807.

Supported by a grant-in-aid for Scientific Research on Priority Area from the Ministry of Education, Science, Sports and Culture of Japan; Health Sciences Research Grants of The Ministry of Health, Welfare and Labor; The Program for Promotion of Fundamental Studies in Health Sciences of the Organization for Drug ADR Relief, R&D Promotion and Product Review of Japan; and grant from The Sankyo Foundation of Life Science.

Y.S. and H.F. contributed equally to this work.

臨　床

HIV・HCV重複感染症の現状

塚田訓久，小池和彦*
東京大学医学部附属病院　感染症内科（*科長）

重複感染の疫学

2003年末の時点で，全世界で約4,000万人がヒト免疫不全ウイルス(human immunodeficiency virus；HIV)に感染していると推測されている[1]．国内での感染者数も年々増加しており，非加熱凝固因子製剤などの血液製剤投与による感染例(血友病例を代表とするいわゆる「薬害エイズ」例：以下血友病例)を除いて，2003年末までの累計で9,000人近くが報告されている(厚生労働省エイズ動向委員会)．感染に気付いていない例も含めると，さらに多くの感染者が存在すると考えられる．

HIVは血液・体液を介して感染するため，同様の経路で感染するC型肝炎ウイルス(hepatitis C virus；HCV)との重複感染が生じ得る．海外からの報告では，HIV感染者のうちかなりの割合がHCVに重複感染しているとされる(2000年のGreubらの報告[2]では37.2%，2002年のSulkowskiらの報告[3]では44.6%など)．ただし，2003年までに国立国際医療センターエイズ治療・研究開発センター(AIDS Clinical Center；ACC)を受診した症例に関する筆者の検討(2003年エイズ学会報告)では，国内のHIV感染者のHCV重複感染率は，血友病例を除けば5%程度であり，海外と比較して低い．

国内で重複感染率が低い真の理由を知ることは難しいが，HIV感染の主要な経路(血液製剤による感染を除く)は性行為によるものと静注薬物濫用に伴うものであり，一般に前者でのHCV感染リスクは低く，後者ではきわめて高い．厚生労働省エイズ動向委員会の報告によれば，報告された平成15年度の新規感染者の8割以上が性行為による感染者であり，静注薬物濫用によるものは1%未満と考えられていることから，静注薬物濫用の頻度の差が重複感染率の差に影響していると推測できる．

血友病例においては，HIVに感染している例のほとんどがHCVにも重複感染しており，総数においても国内でのHIV・HCV重複感染例のかなりの割合を占めると考えられる．

重複感染の問題点

HIV・HCV重複感染の問題点を考える際は，HIVの重複感染がHCV感染症に与える影響と，HCVの重複感染がHIV感染症に与える影響に分けて考える必要がある(表1)．

HIVの重複感染がHCV感染症に与える影

表 1. 重複感染の相互作用

HIV 重複感染の HCV 感染症への影響	HCV 重複感染の HIV 感染症への影響
・肝線維化の進行が速くなる. ・インターフェロン療法の成績が低下する. ・抗 HIV 薬の長期毒性がリバビリンにより増強される可能性がある.	・HIV 感染症の進行には影響しない(これに反対する意見もある). ・抗 HIV 薬による肝機能障害がより高頻度に出現する.

響としては，①HIV の重複感染により肝線維化の進行が速くなる[4]，②HIV の重複感染例では，HCV 単独感染例と比較してインターフェロン(IFN)療法の有効性が低い，が挙げられる.

HCV の重複感染が HIV 感染症に与える影響については，重複感染例で AIDS 指標疾患の発症率・死亡率がより高いとする報告もときにみられるが，影響しないとする意見が現在の主流である. ただし，HCV 重複感染例では，HIV 単独感染例と比較して抗 HIV 薬による肝障害がより高頻度に出現することが知られている.

最近では，抗 HIV 療法の進歩に伴い，日和見疾患のために死亡する HIV 感染者数は減少している. とくに血友病例は，いわゆる「非加熱製剤」が流通していた時期，すなわち 1980 年代までに HIV・HCV に重複感染しており，感染から約 20 年を経過していることから，C 型肝炎・肝硬変が生命予後を規定する最大の因子となりつつある.

重複感染例の現状

筆者による 2003 年現在 ACC に通院中の重複感染例の検討では，血友病例以外の症例で，①HIV 感染症のコントロールはより良好で，②肝機能も良好に保たれている例が多かった. この理由として，血友病例以外の症例の多くが 1997 年頃，すなわち HIV 感染症に対する 3 剤併用療法(highly active anti-retroviral therapy；HAART)が広く行われるようになった時期以降の HIV 感染例であり，最初から有効な抗 HIV 療法を行うことが可能であったこと，HCV 感染からの期間が血友病例と比較して短いことが考えられる. 非代償性肝硬変と判断される例は血友病例で 7 例，それ以外の例で 2 例であったが，後者の 2 例はいずれも 50 歳以上であり，HIV に感染したことが推定される時期よりも前に HCV に感染していたことが疑われ，HCV の感染経路と HIV の感染経路が同一であるか否かについても不明であった.

2001 年エイズ学会における矢崎らの報告によれば，1997 年以降に ACC で死亡した症例を検討した結果，血友病例の半数(6 例中 3 例)が肝硬変・肝細胞癌による死亡であり，残り 3 例中 2 例でも進行性肝疾患の所見がみられたのに対し，それ以外の原因による HIV 感染例(HCV 重複感染例とは限らない)の死亡原因は，そのほとんど(12 例中 11 例)が日和見疾患による死亡(いわゆる「エイズ死」)であった. このことから，少なくとも血友病例においては，日和見疾患より C 型肝炎関連疾患が現在より大きな問題であると考えることができるだろう.

重複感染の治療：HIV

HIV 感染症の治療の目標は，抗 HIV 薬を使用して体内での HIV の増殖を可能な限り抑制し，これにより HIV による細胞性免疫システムの破壊を抑制することである. この目標自体は，HIV・HCV 重複感染例においても変わらない.

現在のHIV感染症の標準的治療は，3剤以上の抗HIV薬を組み合わせて行う，いわゆるHAARTである．現在使用可能な抗HIV薬はおおまかに，核酸系逆転写酵素阻害薬(nucleoside reverse transcriptase inhibitor；NRTI)，非核酸系逆転写酵素阻害薬(non-nucleoside reverse transcriptase inhibitor；NNRTI)，プロテアーゼ阻害薬(protease inhibitor；PI)の3系統に分類され，通常は二種類のNRTIに1種類のNNRTIあるいはPIを組み合わせた3剤が選択される(詳細は成書および最新のガイドラインを参照のこと)．

重複感染例におけるHIV感染症治療で考慮すべき点として，前述のように薬剤性肝障害がより高頻度に発生することが挙げられる．肝障害が理由で有効であるはずの抗HIV療法を継続できない例も存在することから，これは大きな問題である．2003年のPuotiらの報告[5]によれば，IFNによるC型肝炎の先行治療によって，HAARTによる肝障害の発生を抑えることが可能であった．これは，この肝障害に細胞性免疫能の改善によりそれまで見かけ上沈静化していたC型肝炎が顕在化する，いわゆる「免疫再構築症候群」が関与している可能性を示唆する．

重複感染の治療：HCV

HCVを体内から排除できる可能性のある治療法として，現時点で広く利用できるのはIFN投与のみであり，リバビリンの併用によりその治療効果は増強される．

2000年のLandauらの報告[6]以降，HIV・HCV重複感染例においてもリバビリン併用療法の報告が相次いでおり，現在では主流となっている．ただしその治療成績については，重複感染例においてもリバビリン併用によりIFN単独投与による治療と比較して治療成績は改善されるものの，HCV単独感染例との比較では重複感染例で治療成績が劣るとするものが多い．我が国では欧米諸国と比較してIFN投与量が多くリバビリン投与量が少なめであるという違いがあるが，治療成績についてはおおむねこのような傾向を示す．HCV単独感染例より劣る治療成績の理由として，HIV感染による細胞性免疫能の障害や，(一部関係するが)高いHCV-RNA量などが考えられている．

HIV・HCV重複感染例における併用療法の問題点として，①血球減少などIFNによる副作用がHCV単独感染例と比較して強く出る可能性がある，②IFN使用中はCD4陽性Tリンパ球数が低下する(ただしこれは必ずしも日和見疾患の増加とは関連しないとされる)，③NRTIとリバビリンの併用によりNRTIの副作用(ミトコンドリア障害によるとされるもの)が増強される可能性がある，などが挙げられる．

現在ではPEG-IFNの導入など新たな試みが行われており，その治療成績が注目される．ただし我が国の現状として，現在でもHCVによる活動性肝炎が残存している血友病例には，過去にIFN投与による治療を試みたものの副作用のため完遂できなかった例，過去の治療が失敗に終わった例も含まれており，このような症例で今後再度のIFN投与を行った場合の成績はより劣ることが予想される．このような症例に対しては，必要に応じて対症的に肝庇護療法を行っているのが実情であるが，肝線維化の進行は免れない．

重複感染例に対する肝移植：背景

非代償性肝硬変に至った症例では，内科的治療による肝機能の改善は期待できない．腹水・食道静脈瘤・血小板減少など一般的な肝硬変の合併症に加え，HIV重複感染例においては肝予備能の低下のために抗HIV薬の使用に制限が生じることが大きな問題である．また，肝予備能が保たれていても，抗HIV薬の肝障害が強く現れるために有効なHAARTを行うことが

できず，結果として免疫不全が進行する症例もみられる．

肝硬変に対する根治療法は，現時点では肝移植のみである．HCV 抗体陽性例に対する肝移植は世界中で広く行われているが，HIV・HCV 重複感染例においては HCV 単独感染例と比較して，以下に述べるように，より多くの考慮すべき点があり，脳死ドナーの絶対的な不足もあって，ごく限られた施設でしか行われていないのが現状である．我が国においては，2001 年に我々の施設で重複感染例に対する世界初の生体部分肝移植術[7]が行われて以来，本稿執筆時点の 2004 年 6 月までに 5 例の同様の手術が行われている．

重複感染例に対する肝移植：問題点

肝移植後には移植片拒絶の予防・治療のため免疫抑制剤やステロイドが投与され，細胞性免疫が低下した状態にある．このため，移植後にはサイトメガロウイルス(cytomegalovirus；CMV)感染症をはじめとする各種の日和見疾患のハイリスク状態となるが，HIV 感染症の合併によりこのリスクはさらに増大すると考えられる．通常の HIV 感染症診療においては，CD4 陽性 T リンパ球数を免疫能の指標として日和見感染症の検索・予防内服を行うが，移植後においては必ずしも CD4 陽性 T リンパ球数が免疫状態と比例しないため，予防内服については明確な基準がない状態である．実際に我々の施設においても，重複感染例の肝移植術後に CMV 感染症を発症し，最終的に小腸病変からの出血により死亡した例を経験しているが，この例では CD4 陽性 T リンパ球数が比較的高い値を示していた時点ですでに CMV 抗原血症が遷延していた．

肝移植後の C 型肝炎の再発は必発であるが，これに対しては術後 IFN とリバビリンの併用療法が行われる．症例数が少ないためいまだその成績を評価できる段階にはないが，肝移植後においても通常の C 型肝炎治療時と同様 HIV 重複感染例では HCV 単独感染例と比較して効果が低い可能性がある．肝移植後に C 型肝炎が再燃した場合には，HIV の重複感染によりその進行は速くなることが予想される．

重複感染例に対する肝移植：移植後の HIV 感染症治療

肝移植後の HIV 感染症治療に関して大きな問題となるのは，①抗 HIV 薬の肝障害，②抗 HIV 薬と免疫抑制剤の相互作用の 2 点である．とくに生体肝移植の場合には，脳死全肝移植と異なり，術後数週間の間に移植片の容積が急速に増加するが，この期間中に抗 HIV 薬を投与することによる影響はいまだ不明である．また，とくに PI と免疫抑制剤との相互作用は強く，併用によりタクロリムス(tacrolimus)やシクロスポリン(cyclosporine)の血中濃度が数十倍にも上昇するため，免疫抑制剤の血中濃度の微調節を必要とする術後急性期の投与は，可能な限り避けたい．しかし，逆に HAART 開始を遅らせることにより HIV 感染症が進行した場合，日和見疾患を発症するリスクが高くなる．症例ごとに経過が大きく異なるため，明確な基準を作ることは将来的にも難しいことが予想されるが，術後しばらくの間は HAART を行うことができないという前提で(その間の HIV 感染症の進行も視野に入れた上で)，手術適応を判断する必要があるだろう．

術後の抗 HIV 薬選択に関しては，通常の HAART の際の薬剤選択と同様，耐性のない薬剤から 3 種類を選択することが原則となる．しかし実際には，血友病例では過去に長期間の薬剤投与歴を有するものが多く，単剤投与の繰り返しにより複数の薬剤に耐性を獲得している場合も珍しくない．また，外科的合併症などさまざまな理由により，一時的に抗 HIV 薬の投与を中止せざるを得ない場合があり，これにより HIV が耐性を獲得してしまう可能性もある．過

去に耐性を獲得していない薬剤を中心に最も有効と考えられる治療薬を組み合わせることになるが，周術期の合併症(腎機能障害・貧血など)により，術前に予定していた薬剤を使用できなくなる可能性があることに注意が必要である．術後に使用できる有効と考えられる抗HIV薬が存在しない場合は，新規薬剤の開発状況と合わせ移植自体の適応を再検討する必要があるだろう．

このように，重複感染例に対する肝移植についてはその長期成績も含めいまだ不明な点もあるが，実際に移植が成功した例においては，生命予後は勿論のこと，その生活の質の改善には著しいものがあり，IFNが無効で将来的に非代償性肝硬変に至ることが予想される例では，治療法の一つとして考慮すべきものと考える．

文　献

1) UNAIDS Website (http://www.unaids.org/)
2) Greub G *et al*：Clinical progression, survival, and immune recovery during antiretroviral therapy in patients with HIV-1 and hepatitis C virus coinfection: the Swiss HIV Cohort Study. Lancet **356**：1800, 2000.
3) Sulkowski MS *et al*：Hepatitis C and progression of HIV disease. JAMA **288**：199, 2002.
4) Benhamou Y *et al*：Factors affecting liver fibrosis in human immunodeficiency virus-and hepatitis C virus-coinfected patients: impact of protease inhibitor therapy. Hepatology **34**：283, 2001.
5) Puoti M *et al*：Severe hepatotoxicity during combination antiretroviral treatment: incidence, liver histology, and outcome. J Acquir Immune Defic Syndr **32**：259, 2003.
6) Landau A *et al*：Efficacy and safety of combination therapy with interferon-alpha2b and ribavirin for chronic hepatitis C in HIV-infected patients. AIDS **14**：839, 2000.
7) Sugawara Y *et al*：Living-donor liver transplantation in an HIV-positive patient with hemophilia. Transplantation **74**：1655, 2002.